

**Towards a Lagrangian Ocean Model: Simulating Upwelling  
in a Large Lake Using Slippery Sacks**

*Patrick T. Haertel*

Cooperative Institute for Research in Environmental Sciences, University of Colorado  
NOAA Aeronomy Laboratory, Boulder, Colorado

*David A. Randall*

Department of Atmospheric Science, Colorado State University

*Tommy G. Jensen*

International Pacific Research Center, University of Hawaii at Manoa

7 November 2002

---

*Corresponding author address:* Dr. Patrick T. Haertel, NOAA Aeronomy Laboratory  
R/AL3, 325 Broadway, Boulder, CO 80305-3328 E-mail: phaertel@al.noaa.gov

## ABSTRACT

A Lagrangian numerical model is used to simulate upwelling in an idealized large lake. This simulation is carried out to test the model's potential for simulating ocean circulations.

The model is based on the Slippery Sack (SS) numerical method, which was recently developed by the authors. It represents the lake as a pile of sacks having no vertical gaps. The horizontal motions of the sacks are prognosed using Newtonian dynamics. The model uses Gravity Wave Retardation to allow for long time steps and has pseudo-Eulerian vertical mixing.

The lake is exposed to northerly winds for 29 hours. Upwelling develops in the eastern edge of the basin, and after the winds shut off upwelling fronts propagate around the lake. This case was previously simulated using a height- and a sigma-coordinate ocean model. The SS simulation, which has half the horizontal resolution of the previous simulations, requires a comparable amount of computer processing to complete. The lake's circulation is similar in all three simulations, but the SS simulation exhibits the least diffusion.

## 1. Introduction

In this study we modify our Slippery Sack (SS) free-surface fluid model (Haertel and Randall 2002, hereafter HR02) and use it to simulate upwelling in an idealized large lake. This simulation is carried out to test the model's potential for simulating ocean circulations. To begin, we review the SS method, motivate the development of an SS ocean model, and explain why we select lake upwelling as a test problem.

### *a. The SS method*

Under the SS method a fluid is represented as a pile of sacks having no vertical gaps (e.g. Fig. 1). Each sack is constrained to lie above other sacks having greater density. Horizontal positions  $\mathbf{x}_i$  and velocities  $\mathbf{v}_i$  of sacks are prognosed using Newtonian dynamics:

$$\frac{d\mathbf{x}_i}{dt} = \mathbf{v}_i \quad (1)$$

$$\frac{d\mathbf{v}_i}{dt} + f \mathbf{k} \times \mathbf{v}_i = \frac{\mathbf{F}_{p_i} + \mathbf{F}_{e_i}}{M_i} \quad (2)$$

where  $i$  is the sack index,  $t$  is time,  $f$  is the Coriolis parameter,  $\mathbf{k}$  is the unit vector in the vertical,  $\mathbf{F}_{p_i}$  the horizontal force on sack  $i$  resulting from pressure,  $\mathbf{F}_{e_i}$  is the horizontal force on sack  $i$  resulting from eddy viscosity, and  $M_i$  is the mass of sack  $i$ . Equations (1-2) are easily stepped forward in time (e.g. by Adams-Bashforth time-differencing); the challenge of solving them is diagnosing  $\mathbf{F}_{p_i}$  and  $\mathbf{F}_{e_i}$ .

Each slippery sack is assumed to have a horizontal mass distribution  $m_i(\mathbf{x}')$  that is constant with respect to time in the sack's frame of reference ( $\mathbf{x}'$  denotes horizontal position relative to the sack center). Each sack is also assumed to have a spatially uniform density  $\rho_i$ . It follows that a sack's vertical thickness  $H_i$  is

$$H_i(\mathbf{x}) = \frac{m_i(\mathbf{x} - \mathbf{x}_i)}{\rho_i}, \quad (3)$$

and the horizontal force on a sack resulting from hydrostatic pressure is

$$\mathbf{F}_{p_i} = \int g \nabla H_i \left[ \sum_{\rho_j < \rho_i} (\rho_j - \rho_i) H_j + \sum_j \rho_i H_j \right] dA \quad (4)$$

where  $A$  is the horizontal area measure (this is a variant of Equation (7) in HR02 that was obtained by rearranging terms). Equation (4) may be approximated with a Riemann sum, which conserves energy in the limit as the time step approaches zero and requires  $O(n)$  operations to evaluate for  $n$  sacks (HR02).

When  $\mathbf{F}_{e_i}$  is set to zero (1-4) form a complete system. HR02 use this system to simulate a non-linear deformation, internal and external gravity waves, and Rossby waves. These simulations serve to test the numerical fidelity of the SS method, and their interpretation is not complicated by the presence of viscous effects. For each test case the SS solutions rapidly converge to analytic and high-resolution finite-difference solutions as the size of the sacks used to represent the fluid is decreased. For example, Fig. 2 shows the dependence of the velocity error on sack size for an SS simulation of gravity waves within a two layer system. The normalized velocity error is approximately proportional to the square of sack width.

Incorporating variable bottom topography into the SS method is easy; one defines the lowest sack to be immobile and to have the shape of the bottom topography. As the reader will soon find out, incorporating viscosity and time-dependent densities into the SS method is also straightforward. The SS method has similarities with both Smoothed Particle Hydrodynamics (Monagan 1992) and oceanic applications of the particle-in-cell method (e.g. Pavia and Cushman-Roisin 1988) as is discussed in HR02.

*b. The potential merits of an SS ocean model*

The SS method has a number of properties that would appear to make it well suited for simulating ocean circulations: (1) in the absence of parameterized mixing it perfectly conserves a fluid's distribution of temperature and salinity; (2) the inclusion of continuous topography adds no numerical complexity to the SS method; (3) the SS method is capable of representing a continuum of fluid densities; and (4) the SS method can represent vertical variations in neutral regions. Property (1) distinguishes an SS model from both height- and sigma-coordinate ocean models, which produce spurious mixing (Griffies et al. 2000). Property (2) also distinguishes an SS model from height-coordinate ocean models, which either have step topography or represent sloping topography in a complicated manner (e.g. Pacanowski and Gnanadeskikan 1998). Properties (3-4) distinguish an SS model from isopycnal ocean models, which have a discrete set of densities and do not resolve neutral regions (Bleck 1998).

In short, an SS ocean model promises to be unique, both in its capabilities and its simplicity. Therefore, we have set out to develop our SS model into an ocean model, a goal that we partially accomplish in the present study.

*c. Lake upwelling, a good test problem*

Rather than immediately applying our SS model to the oceans, which would require using very low resolution or specifying open boundary conditions, we have elected to first test the model with the problem of lake upwelling. We simulate one of the cases considered by Beletsky et al. (1997), who simulated upwelling in idealized large lakes and in Lake Michigan using both a z-coordinate and a  $\sigma$ -coordinate ocean model. The lake, which sits in a paraboloid basin, is exposed to a surface wind-stress forcing that lasts 29 hours. Upwelling develops in response to the forcing, and after the forcing shuts off upwelling fronts propagate around the lake. This case is a good test of SS model's potential for simulating ocean circulations for the following reasons: (1) it is a simple

example of the response of a body of water to a surface wind-stress forcing, (2) the lake has variable bottom topography, (3) the response involves internal gravity wave dynamics and boundary currents, and (4) comparing the SS upwelling simulation to those carried out by Beletsky et al. illustrates differences between SS and  $z$ - and  $\sigma$ -coordinate models.

#### *d. Outline*

This paper is organized as follows. Section 2 discusses two modifications to the SS model that improve computational efficiency. Section 3 describes the model's implementation of vertical diffusion. The upwelling simulation is presented in Section 4. Section 5 is a discussion, and Section 6 is a summary.

## **2. Computing Efficiently**

Modern ocean models push the limits of modern supercomputers (e.g. Smith et al. 2000), so computational efficiency is a high priority for the ocean model developer. This section describes two ways we have modified our SS model to make it more computationally efficient. The first modification reduces the computer time required to evaluate sack thickness functions and their gradients (in order to solve (4)). The second modification lengthens the maximum allowable stable timestep. These modifications have enabled our SS model to complete the upwelling simulation presented later in just 20 minutes on a 2.4 GHz Pentium 4 processor using no optimizations that compromise mathematical accuracy.

#### *a. Using a polynomial mass-distribution function*

The sack mass-distribution function used by HR02 is a cosine-squared bell function, and it was selected because it has several nice properties: (1) it is continuous, (2) it has a continuous horizontal gradient that vanishes at the sack's edges, and (3) it is easy to construct piles that are perfectly level using sacks with this mass distribution.

However, this function is computationally expensive, because computers approximate trigonometric functions using power series that require many floating point operations to evaluate. The following mass-distribution has the same nice properties, but requires fewer floating point operations to evaluate:

$$m(x', y') = \frac{M_i}{r_x r_y} \left[ 1 + \left( 2|x'| - 3 \right) \left( x' \right)^2 \right] \left[ 1 + \left( 2|y'| - 3 \right) \left( y' \right)^2 \right] \quad (5)$$

where  $r_x$  and  $r_y$  are the sack radii in the  $x$  – and  $y$  – directions respectively,  $x' = (x - x_i)/r_x$ ,  $y' = (y - y_i)/r_y$ , and  $m$  is non-zero only for  $|x'| < 1$  and  $|y'| < 1$ . Evaluating this function and its horizontal gradient at a point requires evaluating two third-order polynomials and two-second order polynomials, a task which modern processors accomplish very quickly (e.g. a 2.4 GHz Pentium processor can do this about 43 million times per second). Tests have revealed that using this mass-distribution instead of the cosine-squared bell function changes solutions little, as long the Riemann sum that approximates (4) has a sufficient horizontal resolution (at least 3 points per sack radius).

### *b. Gravity Wave Retardation*

Under the SS method a pile of sacks has a free surface and supports the rapid oscillations of external gravity waves. In order for these waves to be stable one must use a time step on the order of the time it takes a wave to cross a sack radius. Therefore, by reducing the phase speed of external gravity waves, one can increase the maximum stable time step. In this section we show that gravity waves can be slowed under the SS method by Gravity Wave Retardation (GWR), which Jensen (1996, 2001, 2002) used to lengthen time-steps by factors of 4-16 in several ocean simulations. One advantage GWR has over time-splitting, an alternative used in some ocean models (e.g. Bleck and Smith 1990, Ezer and Mellor 1997), is that GWR does not require separate solutions for internal and external modes.

To implement GWR one simply reduces the portion of the pressure force associated with the external mode by a constant factor. In (4) the pressure force is decomposed into internal and external components, associated with the first and second terms in brackets respectively. Multiplying the external component by a positive constant  $\gamma$  yields:

$$\mathbf{F}_{p_i} = \int_{H_i} g \nabla H_i \left[ \sum_{\rho_j < \rho_i} (\rho_j - \rho_i) H_j + \gamma \sum_j \rho_i H_j \right] dA. \quad (6)$$

Setting  $\gamma < 1$  slows the phase speed of the external mode by the multiple  $\sqrt{\gamma}$  while leaving the phase speeds of internal modes unchanged.

To illustrate the effects of GWR we repeat the gravity wave simulation presented in HR02, using both  $\gamma = 1$  (no GWR) and  $\gamma = 1/2$ . For this test a two-dimensional fluid comprising two 1-m deep layers with densities  $\rho_1 = 1100 \text{ kg m}^{-3}$  and  $\rho_2 = 1000 \text{ kg m}^{-3}$  is initialized with a lower-layer momentum perturbation that has a Gaussian radius of 1 m and an amplitude of 1 cm s<sup>-1</sup>. Gravity is set to 1 m s<sup>-1</sup> and there is no viscosity or rotation. We represent the fluid using 40 sacks for each layer, each having a radius of 1/2 m, and we approximate (3) using a Riemann sum with a resolution of 1/6 m.

For  $\gamma = 1$  the solution (Fig. 3a) is very similar to the one presented in HR02 (see their Figs. 5d,f). This is what we expect, since the only differences between the two simulations are the magnitude of the momentum perturbation, the shape of the mass-distribution function, and the resolution of the Riemann sum used to approximate the pressure equation. The momentum perturbation projects onto both internal and external gravity waves. By 5 s they have propagated away from the center of the domain where the momentum perturbation was originally located (Fig. 3a). The velocity perturbations in the two layers are in (180° out of) phase for the external (internal) waves, as predicted by linear theory (e.g. Gill, 1982, p. 119). When we repeat the simulation setting  $\gamma = 1/2$

the external waves are slowed by the multiple  $\sqrt{1/2}$ , but the internal waves propagate at the same speed (Fig. 3b).

One side effect of GWR is that surface height perturbations associated with geostrophically-balanced external-mode circulations are increased by the factor  $\gamma^{-1}$ . For most lake and ocean applications surface height perturbations are small (tens of *cm* in amplitude), and this amplification is not problematic as long as  $\gamma$  is not selected to be too small. For the upwelling simulation we use  $\gamma = 0.02$ , which allows increasing the time-step by a factor of about 7.

### 3. Vertical Diffusion

One way to parameterize vertical transports of momentum and tracers by eddies in an ocean model is to calculate height-dependent coefficients of vertical viscosity and tracer diffusivity from vertical profiles of horizontal velocity and temperature/salinity or density (e.g. Pacanowski and Philander 1981, Large et al. 1994). In this section we present an implementation of vertical diffusion for the SS method that was developed to facilitate the use of such parameterizations.

#### *a. Pseudo-Eulerian Diffusion*

Including vertical diffusion in an Eulerian fluid model is straightforward; e.g. the time rate of change of a tracer  $q$  can be set equal to the difference between diffusive-fluxes into and out of a grid box divided by the amount of mass in the box:

$$\frac{\partial q_i}{\partial t} = \frac{1}{M_i} \left( Q_{i-\frac{1}{2}} - Q_{i+\frac{1}{2}} \right) \quad (7)$$

where  $i$  is the vertical index of a grid point, the half-indexes denote values at locations half-way between grid points (i.e. at the top and bottom of the grid box),  $M_i$  denotes the total mass in the grid box,  $Q$  denotes the vertical diffusive flux, which may be

approximated as follows:

$$Q_{i+\frac{1}{2}} = -k_{i+\frac{1}{2}} \left( \frac{q_{i+1} - q_i}{\Delta z} \right) \rho_{i+1/2} dA \quad (8)$$

where  $k$  is coefficient of diffusion and  $\Delta z$  denotes the difference in the height of grid-points  $i$  and  $i + 1$ .

To implement vertical diffusion under the SS method we simply divide the model domain into vertical columns, associate each sack with the column that its center lies in, and apply the above finite-difference approximation to each column of sacks. We set the column width equal to the sack radius in each dimension,  $\Delta z$  equal to half of the sum of the maximum vertical thicknesses of sacks  $i$  and  $i + 1$  (i.e. the vertical distance that would separate the sack centers if they were perfectly aligned), and  $\rho_{i+1/2} = (\rho_i + \rho_{i+1})/2$ .

#### *b. Diffusion/advection simulation*

To illustrate the above implementation of diffusion, we apply it to a simple problem that involves both diffusion and advection. Consider a two-dimensional fluid 10  $m$  deep and 20  $m$  across on a periodic domain. Suppose that the  $x$ -velocity of the fluid is  $1/2 m s^{-1}$  at the top,  $-1/2 m s^{-1}$  at the bottom, and varies linearly inbetween. Now suppose a tracer is released in the center of the fluid, initially having a Gaussian distribution with a radius of 2  $m$  in each dimension and a maximum value of 10 units.

We compare an SS and a finite-difference solution to this problem. The SS solution uses 200 sacks, each having a radius and a depth of 1  $m$ . The finite difference solution uses 200 points with  $\Delta x = \Delta z = 1 m$ . Both solutions use (7-8) to represent diffusion, forward time differencing with a very small time step (0.001  $s$ ), and  $k = 1 m^2 s^{-1}$ . The finite difference solution uses centered differencing to calculate the horizontal gradient of the tracer.

For both solutions the tracer coverage is sheared horizontally as it spreads vertically (Fig. 4). Owing to advection errors the finite difference solution contains small regions having negative tracer values (Fig. 4b). In the SS solution the tracer is advected slightly more rapidly (Fig. 4c). Overall, however, the two solutions are quite similar, suggesting that using pseudo-Eulerian diffusion under the SS method produces a solution of comparable quality to a standard finite-difference solution with the same resolution.

#### 4. The Upwelling Simulation

In this section we present an SS simulation of upwelling in an idealized large lake. This case was previously simulated using the Princeton Ocean Model (POM, Blumberg and Mellor 1987) and the Dietrich/Center for Air Technology (DIECAST, Dietrich and Ko 1994) model by Beletsky et al. (1997).

##### *a. The setting*

The lake is 100 *m* deep, has a diameter of 100 *km*, and sits in a parabolic basin. The initial temperature distribution is a function of depth only, 20°C above 5 *m*, 5°C below 15 *m*, with a constant temperature gradient between 5 and 15 *m*. The lake is initially motionless and is exposed to northerly winds for 29 hours. The amplitude of the wind-stress starts at zero, ramps up to 0.3  $N\ m^{-2}$  over 18 *h*, maintains this value for 6 *h*, and ramps to zero over the next 5 *h*.

##### *b. Initialization*

The SS model is initialized by the following procedure. The lake's domain, a box 100 *km* across in each horizontal dimension and 100 *m* deep, is divided into rectangular columns having widths  $dx = dy = 2.5\ km$ . Each column is divided into a stack of 28 boxes with the following vertical dimensions: 6 at 10 *m*, 2 at 5 *m*, 4 at 2.5 *m*, 4 at 1.5 *m*, 6 at 4/3 *m*, and 6 at 1 *m* (listed in ascending order). Each box whose center lies above the

lake's bottom is converted to a sack having the same volume as the box and the same horizontal position and temperature as the center of the box. The sack is assigned the horizontal mass distribution defined by (5) with  $r_x = r_y = 2.5$  km. When the sacks are stacked in the parabolic basin, the lake's surface and isotherms are quite wavy (Fig. 5a). A 30-day preliminary simulation is run with Newtonian damping of velocity with a time scale of 1 day in order to allow the sacks to settle and the isotherms to flatten (Fig. 5b).

The effective horizontal resolution of the SS simulation is half that of the POM and DIECAST simulations. The SS and DIECAST simulations have similar vertical resolutions, slightly more than twice that of the POM simulation (Beletsky et al. 1997).

### *c. Numerical Details*

The duration of the simulation is 15 days (as in Beletsky et al. 1997), although we only present results for the first 5 days. Equations (1-2, 3, 5, 7-8) are solved using split time-differencing. The pressure acceleration in (2) is approximated using 3rd order Adams-Bashforth time-differencing with a time-step of 200 s. In order to calculate  $\mathbf{F}_{p_i}$  we approximate (6) using a Riemann sum with a resolution of  $5/6$  km, and we set  $\gamma = 0.02$ . The viscous-momentum and temperature tendencies are prognosed by approximating (7-8) using forward time-differencing with time-steps of 25 to 100 s (shorter time-steps are used during stronger winds for numerical stability). Coefficients of vertical eddy viscosity and tracer diffusion are calculated using the Richardson-number formulation presented in Beletsky et. al. (1997) with  $\alpha = 25 \times 10^{-3} m^3 kg^{-1} s$  and  $K_0 = 10^{-5} m^2 s^{-1}$ . These are the same values used in the DIECAST simulation (W. P. O'Connor, personal communication). The density of each sack is recalculated after each time-step using the UNESCO (United Nations Educational, Scientific, and Cultural Organization) equation of state for pure water. Quadratic bottom friction is included with a coefficient of 0.002. The model is run without horizontal diffusion, but for plotting purposes the cross-sections of temperature (excluding those in the initialization

simulation) are smoothed by applying a running-mean filter having the width of a sack radius in each dimension.

#### *d. Results*

The wind-stress forcing produces an Ekman layer that transports surface water towards the west. By 29 *h* the surface-layer has deepened in the western edge of the basin, and upwelling has developed in the eastern edge (Fig. 6a). The temperature distribution in the SS simulation is similar to the temperature distributions produced by the DIECAST model and POM (Figs. 6b-c, from Beletsky et al. 1997). In the SS solution, however, the water is little cooler in the eastern edge of the basin; the 6°C isotherm intersects the surface a ways off shore (Fig. 6a) whereas in the POM simulation this isotherm intersects the bottom (Fig. 6b) and in the DIECAST simulation it is closer to the shore (Fig. 6c). This difference between the SS and POM and DIECAST simulations is also apparent on horizontal cross-sections of temperature at the depth of 10 *m*; the 6°C isotherm encloses a larger area in the SS simulation (Fig. 7a) than it does in the other simulations (Fig. 7b-c, from Beletsky et al. 1997). The SS solution probably differs in this way from the POM and DIECAST solutions because it has no horizontal diffusion and no numerical vertical diffusion, whereas the POM and DIECAST simulations each have both parameterized and numerical horizontal diffusion in addition to numerical vertical diffusion.

The similarity between the SS and POM and DIECAST solutions persists over time. Fig. 8 shows the temperature distribution at 10 *m* at 120 *h* for each model. In each of the three simulations the upwelling fronts have propagated clockwise around the lake, and the gross structure of the temperature distribution is similar. Once again the SS solution preserves more of the water masses with temperature extremes; both the 6°C and 18°C isotherms enclose larger areas in the SS solution (Fig. 8a) than they do in the POM and DIECAST solutions (Fig. 8b-c, from Beletsky et al. 1997).

Overall the differences between the SS and the POM and DIECAST simulations are small and comparable to the differences between the POM and DIECAST simulations. We conclude that the SS model is capable of simulating the response of a stratified body of water in a basin to a wind-stress forcing, and we remain optimistic about the SS model's usefulness for simulating ocean circulations, especially for applications in which numerical diffusion is detrimental.

## **5. Discussion**

In this section we compare the SS model to other oceans models in light of the results presented in this paper. We also mention how we plan to modify the SS model in the near future.

### *a. Comparisons*

The SS model has advantages over other ocean models related to how it handles physical processes and boundaries, but it is slower than height- and sigma-coordinate ocean models.

#### *1) Advection*

The chief advantage of the SS model is that it has no advection errors. This means there is no numerical mixing of temperature, salinity, or momentum. While this characteristic of the model certainly distinguishes it from height- and sigma-coordinate ocean models, it also distinguishes it from isopycnal models, which have horizontal advection errors.

## *2) Vertical Mixing*

The SS model currently uses pseudo-Eulerian vertical mixing. This means that any vertical mixing scheme used in a height-coordinate model may be adapted to the SS model. One advantage this gives the SS model over isopycnal models is the ability to resolve the mixed layer.

## *3) Bottom topography*

The SS model represents continuous bottom topography in a simple way. This distinguishes it from height-coordinate models that either use step topography or somewhat complicated approximations of continuous topography (e.g. Pacanowski and Gnanadeskikan 1998).

## *4) Lateral Boundaries*

Most ocean models have fixed lateral boundaries. This is unrealistic in the sense that if the water is sufficiently perturbed by a large-scale forcing (e.g. as in tides) it can slosh and significantly change its horizontal boundaries. Models that do allow wetting and drying over tidal flats require rather complicated and costly numerical schemes (e.g. Kowalik and Murty 1993). In contrast, the SS model can naturally represent such wetting and drying, simply by moving sacks up and down the sloping sea bed.

## *5) Computational Efficiency*

One disadvantage of the SS model is that it is slower than height- and sigma-coordinate ocean models, i.e. it must be run at a lower horizontal resolution to require comparable computer processing. For example, the POM simulation would take on the order of 10 minutes to run on a 2 Ghz Pentium processor (D. J. Schwab, personal communication), i.e. a comparable amount of computer processing to the SS simulation,

even though it has twice the horizontal resolution. However, for applications in which numerical diffusion is detrimental the SS model may produce higher quality simulations at a lower resolution (e.g. the SS upwelling simulation exhibits less diffusion than the POM and DIECAST upwelling simulations).

*b. Planned improvements for the SS model*

In the near future we plan to add the following features to the SS model to facilitate the simulation of basin-scale ocean circulations.

*1) Reduced Gravity*

We have begun experimenting with a reduced gravity (e.g. Adamec and O'Brien, 1978) version of the SS model in which the external mode is eliminated completely. This version of the model promises to rapidly carry out simulations in cases where deep water circulations and bottom topography are not important.

*2) Parallel processing*

The SS equations of motion are local, i.e. solving them for a given sack only requires information about conditions within a sack radius in each dimension. Therefore the SS method well-suited to parallel programming, and we have already begun working on a parallel version of the SS model. Each processor will keep track of sacks within a horizontal sub-domain assigned to it. Processors will pass information to each other about sacks within a sack-radius of sub-domain boundaries.

*3) Spherical geometry*

The SS method appears to be easily adapted to spherical geometry. Longitude and latitude may be used as horizontal coordinates for sack positions, and the mass

distribution function may be defined in terms of latitude and longitude deviations from the sack center where the sack radius in each dimension is a fixed number of degrees. Doing so results in a distribution function that has the same form as (5) with the addition of the multiple  $1/\cos(\phi)$  where  $\phi$  is the sack's latitude.

## 6. Summary

In this study we modify our SS model and use it to simulate upwelling in an idealized large lake. Two modifications make the model more computationally efficient: changing the sack mass-distribution function to polynomial form, and using Gravity Wave Retardation to allow for long time-steps. A third modification, including pseudo-Eulerian diffusion, facilitates the use of Richardson-number parameterizations for vertical mixing. The upwelling simulation is similar to two simulations previously carried out with height- and sigma-coordinate ocean models, but it exhibits less diffusion.

The successful completion of the upwelling simulation demonstrates the SS model's potential for simulating ocean circulations. The SS model has several appealing features including no advection errors, a resolved mixed layer, continuous bottom topography, and physical lateral boundaries, although it is somewhat slower than height- and sigma-coordinate models. We continue to modify the SS model and hope to use it to carry out basin-scale ocean simulations in the near future.

*Acknowledgements.* This research was supported by Department of Energy Cooperative Agreement DE-FC02-ER63163 and NOAA Grant GC01-351.

## References

Adamec, D. and J. J. O'Brien, 1978: The seasonal upwelling in the gulf of Guinea due to remote forcing. *J. Phys. Oceanogr.* **8**, 1050-1060.

- Beletsky, D., W. P. O'Connor, D. J. Schwab, and D. E. Dietrich, 1997: Numerical simulation of internal kelvin waves and coastal upwelling fronts. *J. Phys. Oceanogr.*, **27**, 1197-1215.
- Bleck, R., 1998: Ocean modeling in isopycnic coordinates. *Ocean Modeling and Parameterization*. E. P. Chassignet and J. Vernon, Eds., Klaver Academic, 423-448.
- Bleck, R. and L. Smith, 1990. A wind-driven isopycnic coordinate model of the north and equatorial Atlantic Ocean. 1. Model development and supporting experiments. *J. Geophys. Res.* **95C**, 3273-3285.
- Blumberg A. F. and G. L. Mellor, 1987: A description of a three-dimensional coastal ocean circulation model. *Three-dimensional Coastal Ocean Models, Coastal and Estuarine Sciences*, Vol. 4, N. S. Heaps, Ed., Amer. Geophys. Union, 1-16.
- Dietrich, D. E. and D.-S. Ko, 1994: A semi-located ocean model based on the SOMS approach. *Int. J. Numer. Methods. Fluids*, **19**, 1103-1113.
- Ezer, T. and G. L. Mellor, 1997: Simulations of the Atlantic Ocean with a free surface sigma coordinate model. *J. Geophys. Res.*, **102**, 15,647-15,657.
- Gill, A. E., 1982: Atmosphere-ocean dynamics. Academic Press, Orlando, 662 pp.
- Griffies, S. M., R. C. Pacanowski, and R. W. Hallberg, 2000: Spurious diapycnal mixing associated with advection in a z-coordinate ocean model, *Mon. Wea. Rev.*, **128**, 538-564.
- Haertel, P. T. and D. A. Randall, 2002: Could a pile of slippery sacks behave like an ocean? *Mon. Wea. Rev.* (in press).
- Jensen, T. G., 1996: Artificial retardation of barotropic waves in layered ocean models. *Mon. Wea. Rev.*, **124**, 1272-1283.

- Jensen, T. G., 2001: Application of the GWR method to the tropical oceans. *Mon. Wea. Rev.*, **129**, 470-484.
- Jensen, T. G., 2002: Barotropic mode errors in an Indian Ocean model associated with the GWR method. *Global and Planetary Change*, **764**, 1-18.
- Kowalik, Z. and T. S. Murty, 1993: Numerical Modeling of Ocean Dynamics. World Scientific, New Jersey, 481 pp.
- Large, W. G., J. C. McWilliams and S. C. Doney, 1994: Oceanic vertical mixing: A review and a model with a nonlocal boundary layer parameterization. *Rev. Geophys.*, **32**, 363-403.
- Monaghan, J. J., 1992: Smoothed particle hydrodynamics. *Annu. Rev. Astron. Atrophys.*, **30**, 543-574.
- Pacanowski, R. C. and S. G. H. Philander, 1981: Parameterization of vertical mixing in numerical models of tropical oceans. *J. Phys. Oceanogr.*, **11**, 1443-1451.
- Pacanowski, R. C. and A. Gnanadesikan, 1998: Transient response in a z-level ocean model that resolves topography with partial cells. *Mon. Wea. Rev.*, **126**, 3248-3270.
- Pavia, E. G., and B. Cushman-Roisin, 1988: Modeling of oceanic fronts using a particle method. *J. Geophys. Res.*, **93**, 3554-3562.
- Smith, R. D., M. E. Maltrud, R. O. Bryan, and M. W. Hecht, 2000: Numerical simulation of the north atlantic ocean at  $1/10^\circ$ . *J. Phys. Oceanogr.*, **30**, 1532-1561.

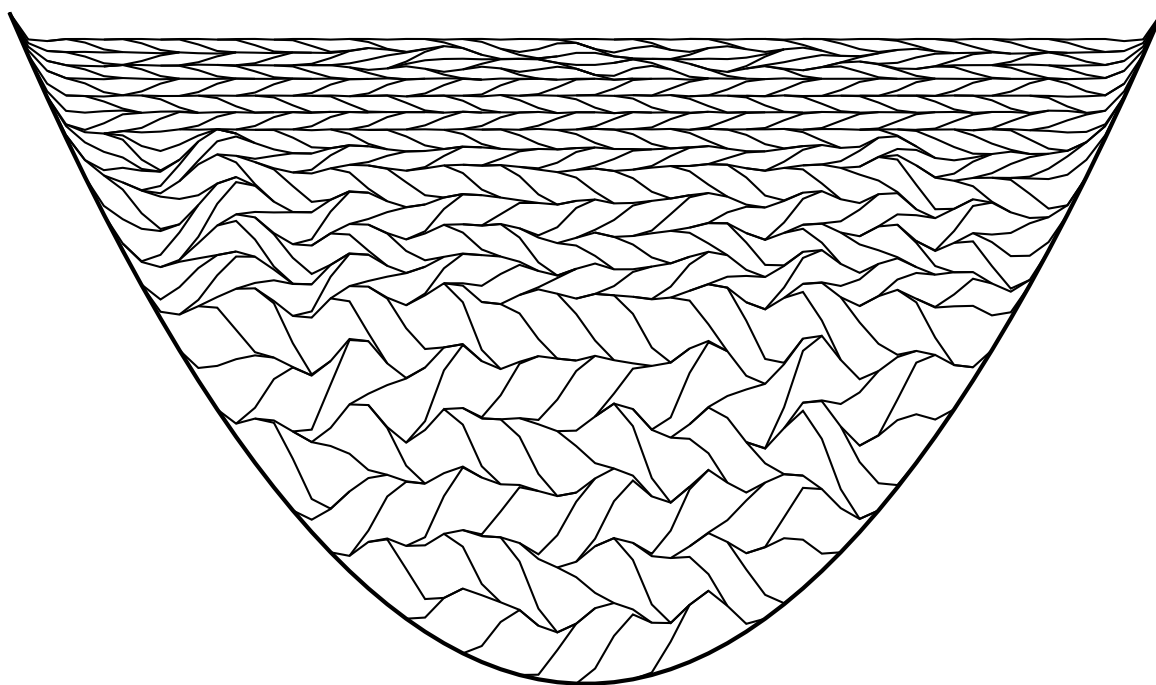


Figure 1. A pile of slippery sacks in a basin.

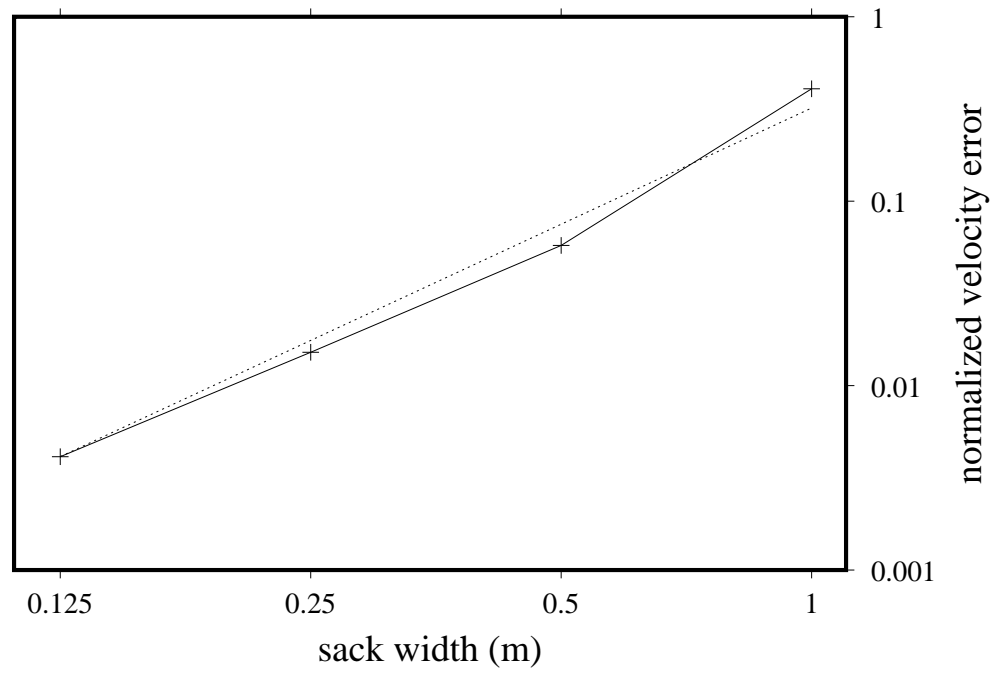


Figure 2. Velocity error as a function of sack size for an internal gravity wave simulation (from HR02). The dotted line has a slope of -2.

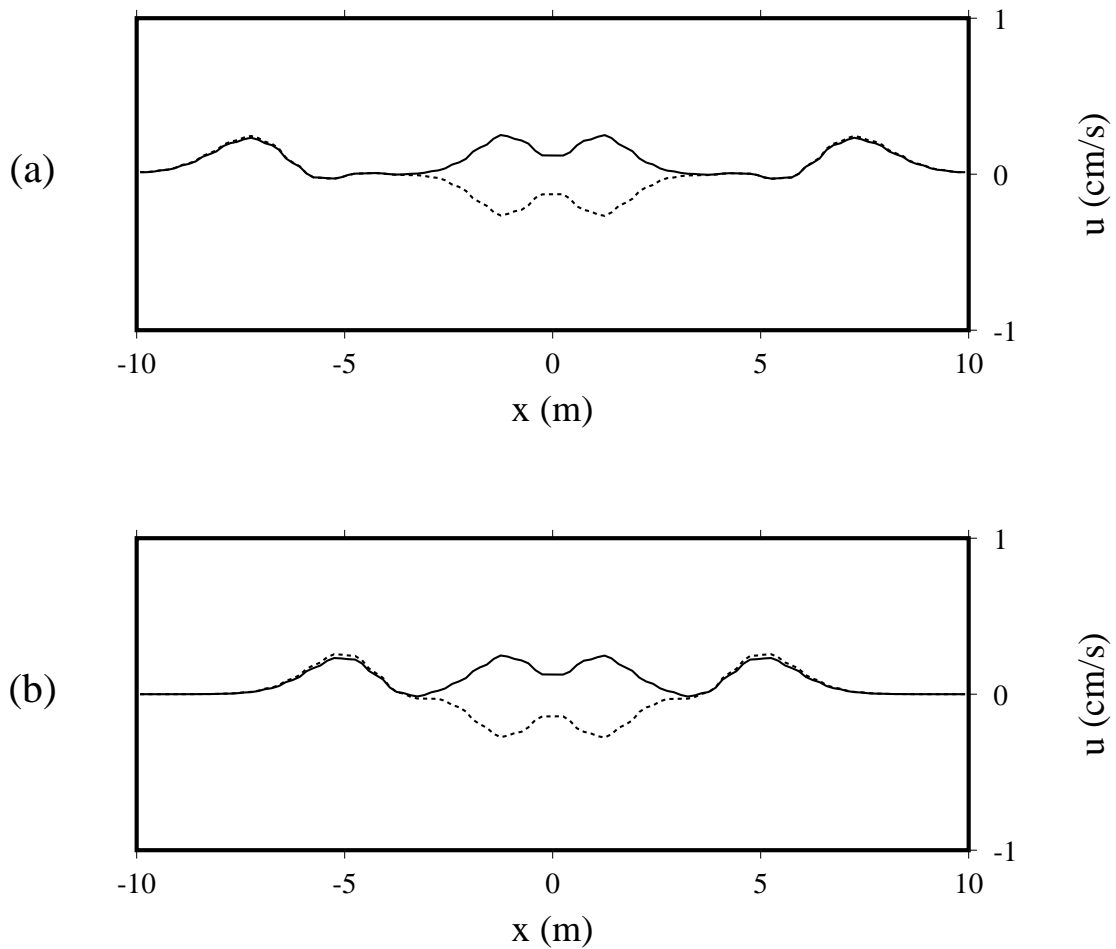


Figure 3. An internal gravity wave simulation that illustrates the effects of GWR. Velocity of the lower (solid) and upper (dashed) layers at 5 s for (a)  $\gamma = 1$  and (b)  $\gamma = 1/2$ .

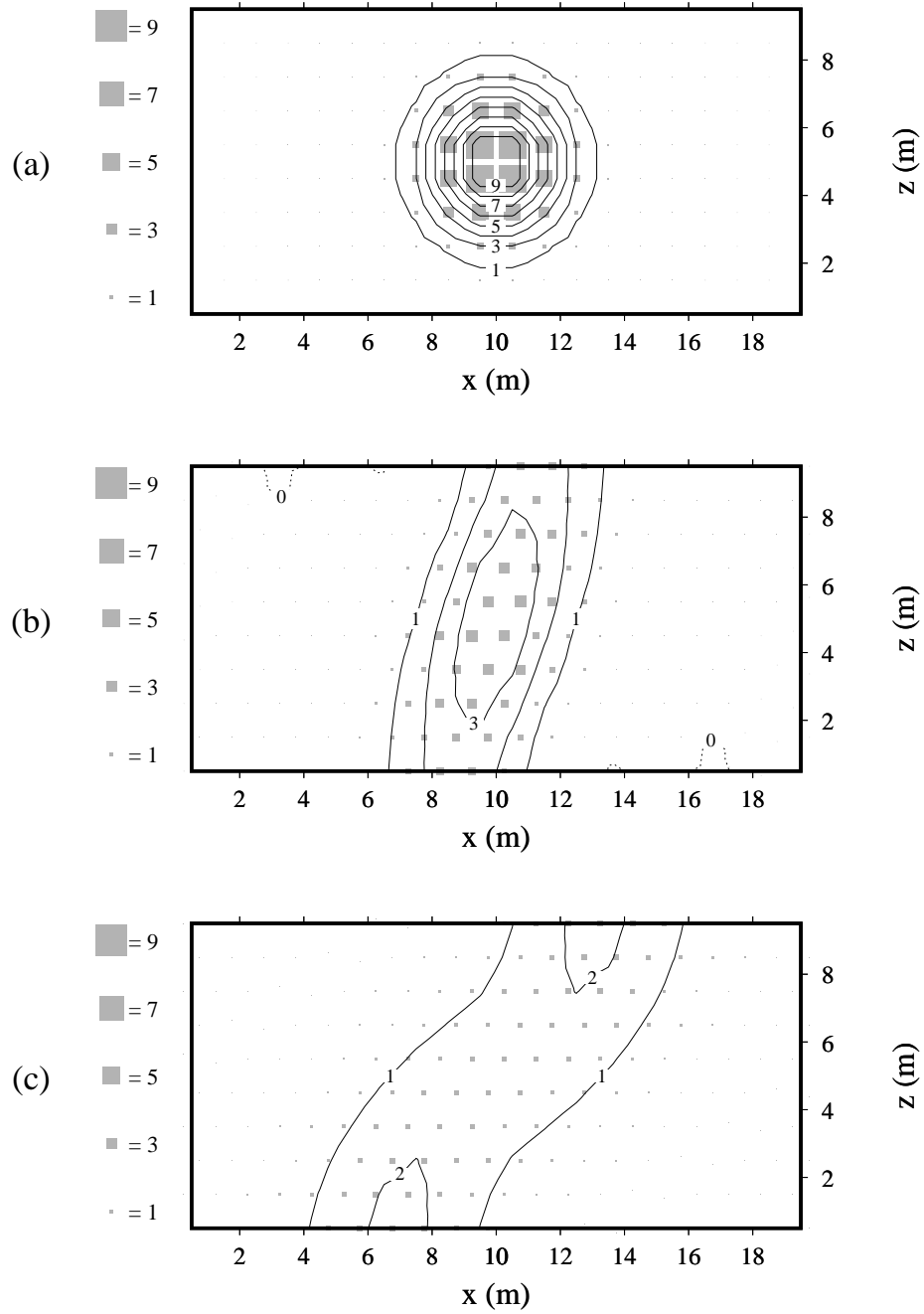


Figure 4. The diffusion/advection simulation. The tracer concentration for the finite-difference solution is contoured with an interval of 1 tracer unit. Centers of sacks in the SS solution are marked with boxes having sizes proportional to the tracer values. The times shown are (a) 0 s, (b) 5 s, and (c) 15 s.

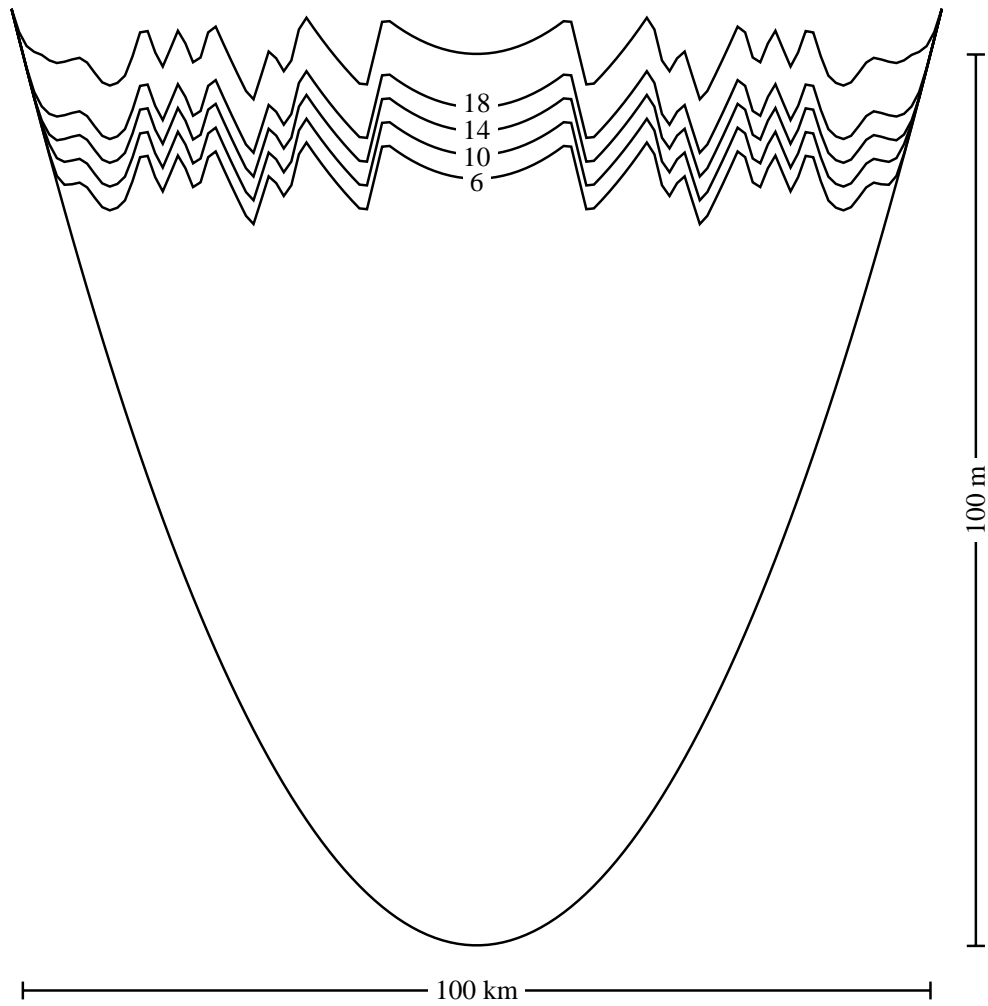


Figure 5. Vertical cross-sections of temperature through the center of the lake for the initialization simulation. (a) 0 days

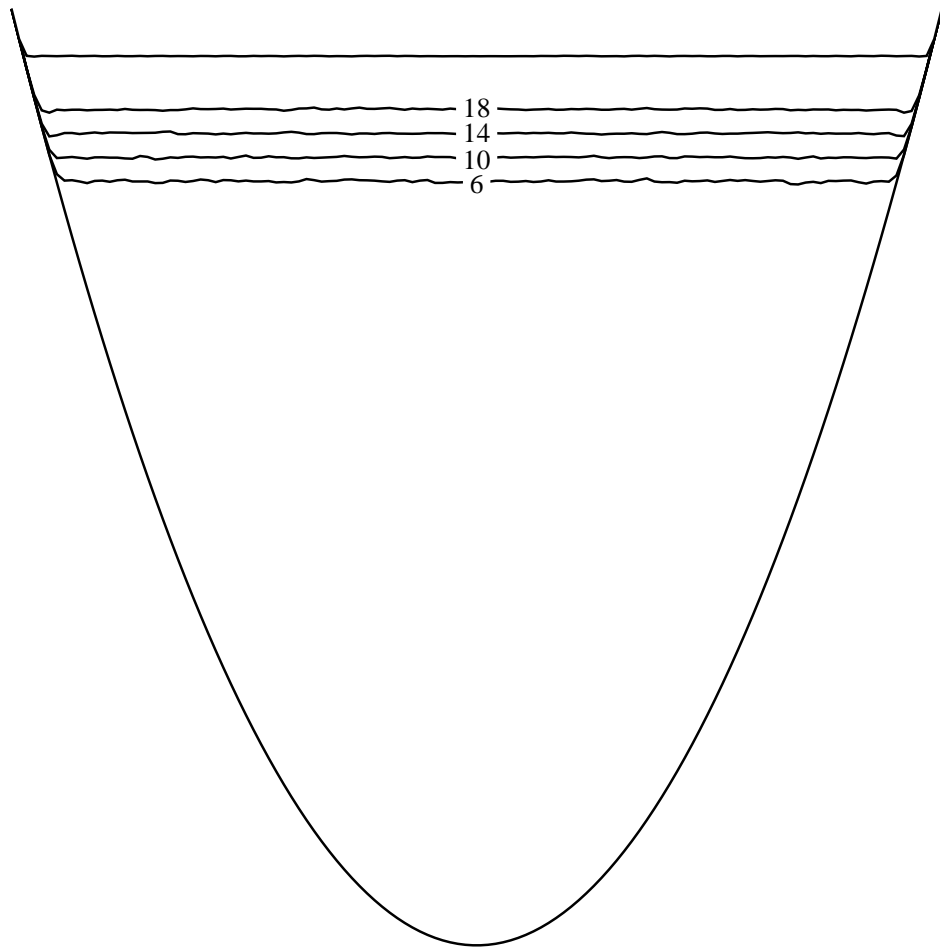


Figure 5 (continued). (b) 30 days.

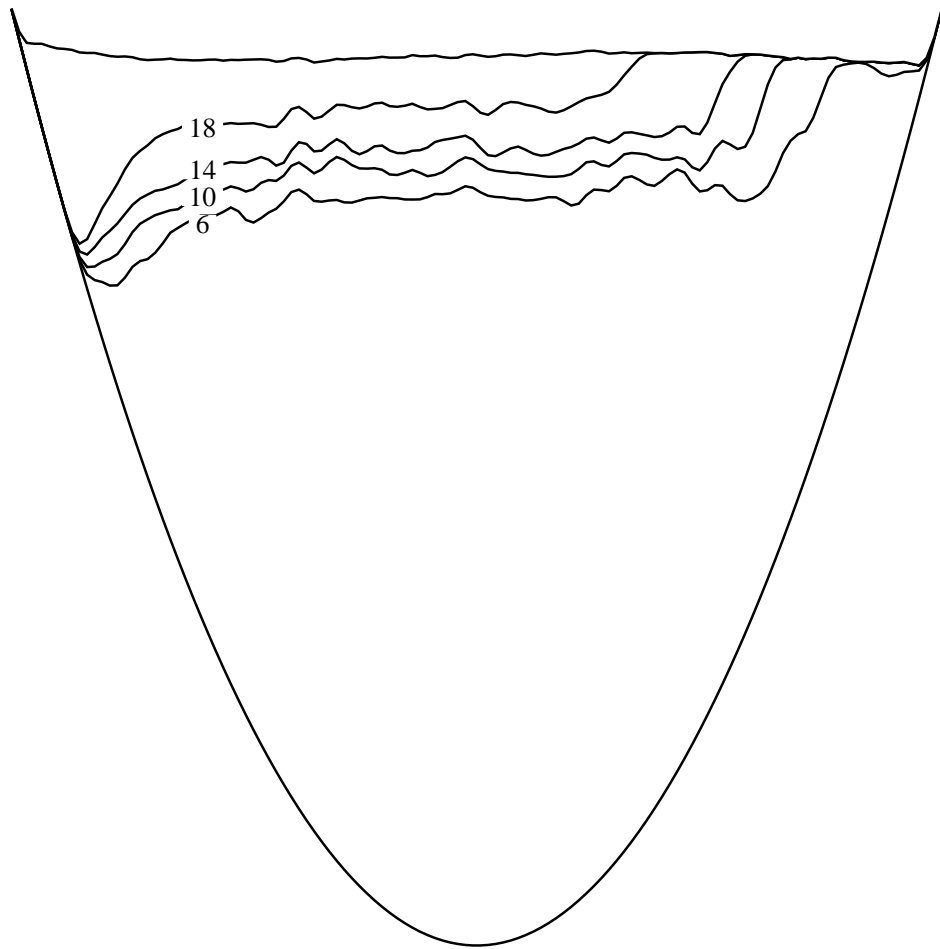


Figure 6. Vertical cross-sections of temperature through the center of the lake at 29 *h*. (a) the SS simulation.

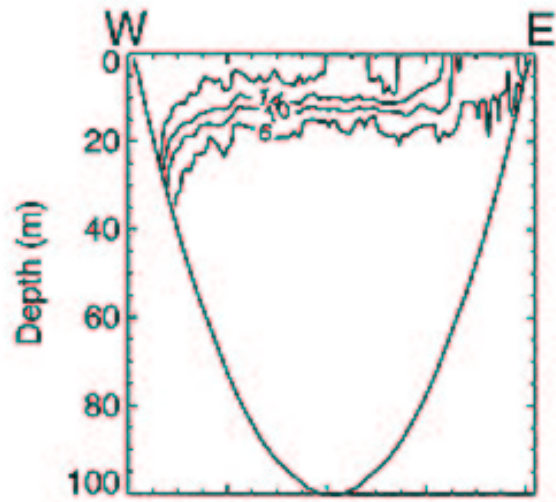


Figure 6 (continued). (b) the POM simulation (from Beletsky et. al 1997).

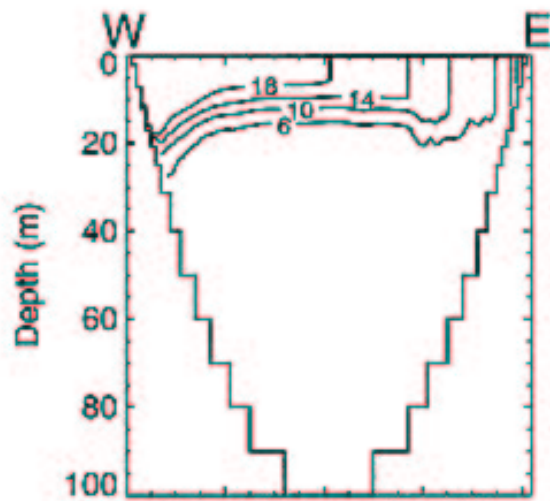


Figure 6 (continued). (c) the DIECAST simulation (from Belestky et al 1997).

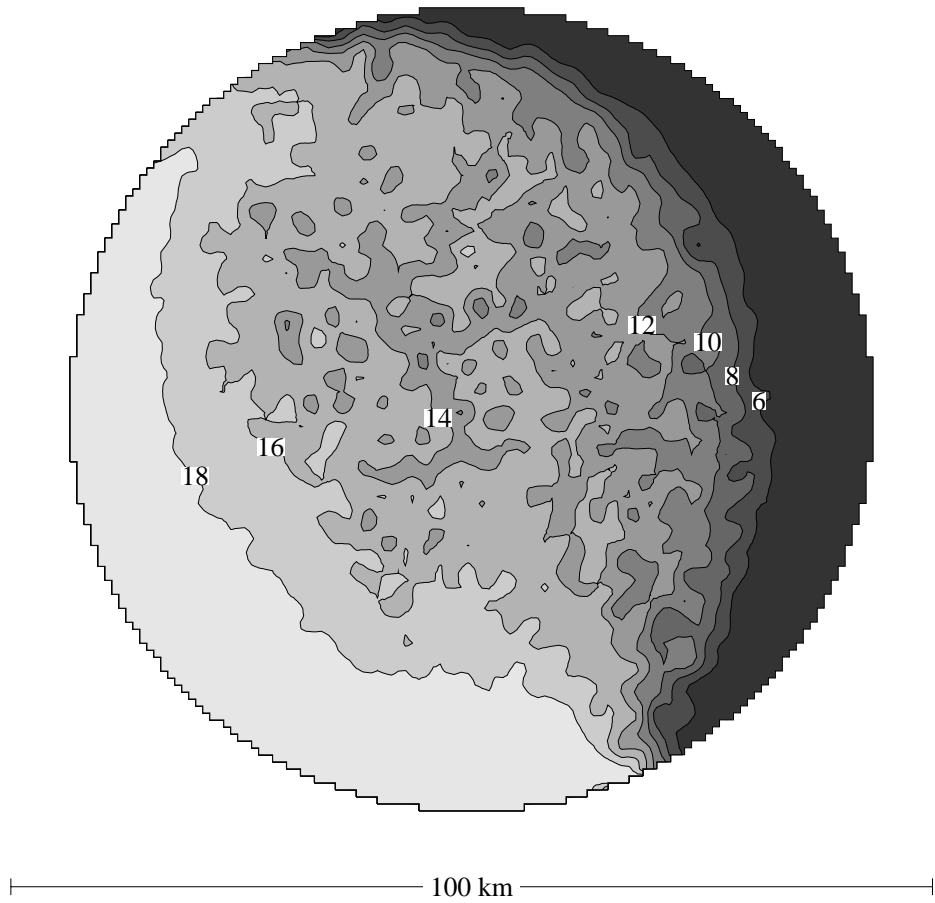


Figure 7. Horizontal cross-sections of temperature at 10 *m* at 29 *h*. (a) the SS simulation.

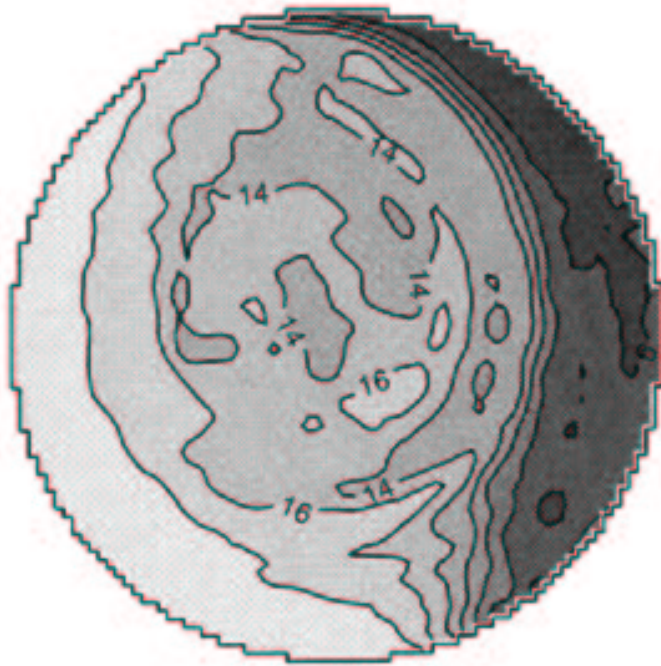


Figure 7 (continued). (b) the POM simulation (from Beletsky et al. 1997).



Figure 7 (continued). (c) the DIECAST simulation (from Beletsky et al. 1997).

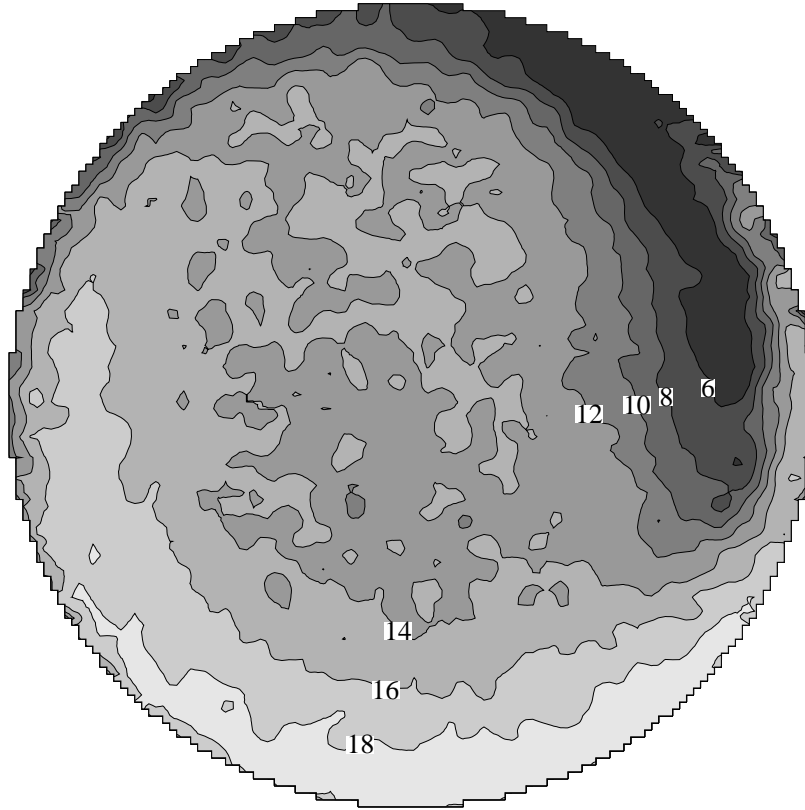


Figure 8. Horizontal cross-sections of temperature at 10 *m* at 120 *h*. (a) the SS simulation.

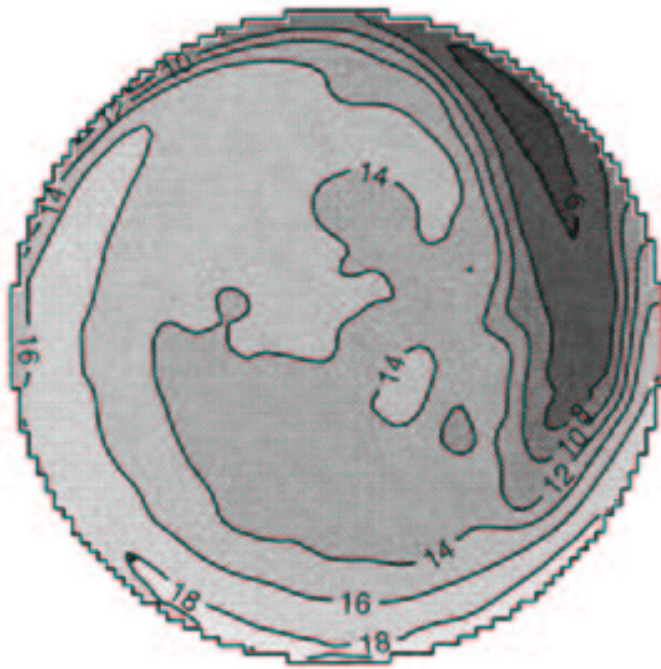


Figure 8 (continued). (b) the POM simulation (from Beletsky et al. 1997).

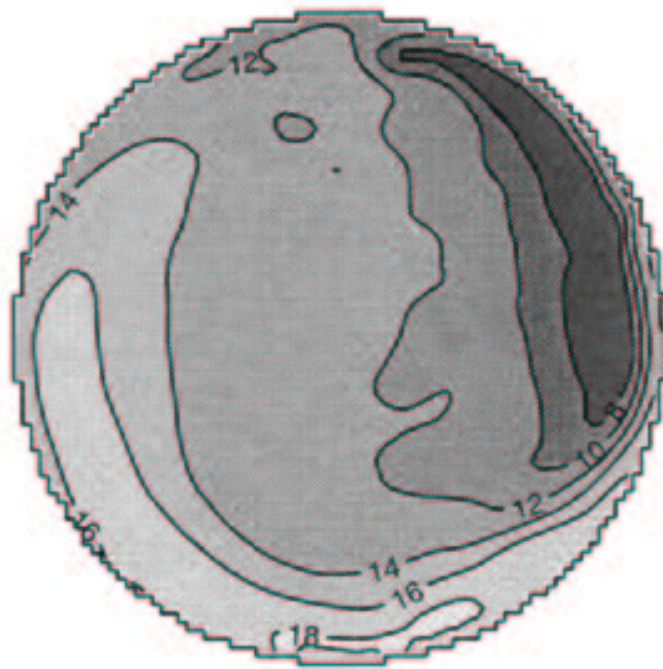


Figure 8 (continued). (c) the DIECAST simulation (from Beletsky et al. 1997).